Gated Electron Transfer: When Are Observed Rates Controlled by Conformational Interconversion?

Brian M. Hoffman* and Mark A. Ratner*

Contribution from the Department of Chemistry, Northwestern University, Evanston, Illinois 60208. *Received February 4, 1987*

Abstract: We explore the consequences that arise when long-range intramolecular electron transfer (ET) occurs in a system that exhibits several *stable* conformational states that can interconvert at rates competitive with electron transfer. Section I recalls the kinetic scheme appropriate for conventional intramolecular ET where reactant and product each exhibit a single stable conformation. Section II discusses the role of conformational dynamics and then proceeds to develop the kinetic scheme that applies to a two-state system in which electron transfer is energetically and kinetically coupled to the conversion between two stable conformations. Section III presents the solution of the corresponding kinetic equations and analyzes their most interesting limiting forms. We find that changes in conformation can entirely alter both the rate and the mechanism of electron-transfer processes in these systems, and thus interpretations of kinetic measurements that ignore such phenomena can be dramatically in error. These results are applied to the task of disentangling electron-transfer and conformational influences on systems of current interest.

Long-range intramolecular electron-transfer processes are the subject of intense current interest.[1] Systems have been synthesized in which (i) a donor–acceptor, [**d**,**a**], redox pair is attached by a rigid covalent linkage[2] and (ii) a redox site is bound to a known position on the surface of a metalloprotein.[3] (iii) Techniques have been developed within our own laboratory,[4] as well as others,[5] to study electron transfer between proteins of an electron-transfer complex. In the present paper we explore the consequences that arise when the system in question exhibits several *stable* conformational states that can interconvert at rates competitive with electron transfer. In particular, we address situations that involve a few major conformational states, such as the classical two-state model of hemoglobin function,[6a] not the case of multiple, similar conformations.[6b] Note that the problem of conformational gating is by no means limited to electron-transfer reactions and has, for example, been considered in the context of CO binding to heme proteins and rotational isomerization of protein aromatic residues.[6c–h] Not surprisingly, we find that conformational interconversion can entirely alter both the rate and the mechanism of electron-transfer processes in these systems, and thus interpretations of kinetic measurements that ignore such phenomena can be dramatically in error.

In section I we recall the kinetic scheme appropriate for conventional intramolecular electron transfer (ET), where reactant and product each exhibit a single stable conformation and conformational dynamics are not important. In section II we discuss the role of conformational dynamics and then proceed to develop the kinetic scheme that applies to a system in which electron transfer is coupled to the conversion between two stable conformations. In section III we solve these equations and analyze their most interesting limiting forms. Finally, the Discussion applies these results to the task of disentangling electron-transfer and conformational influences on systems of current interest.

I. Conventional Intramolecular Electron Transfer

A general kinetic scheme for simple intramolecular electron-transfer reactions is given in Figure 1. A system consisting of an intramolecular (linked) donor–acceptor, [**d**,**a**], pair in its ground state, A, is excited to a reactive state, A*. Most often this is done by flash photolytic excitation of **d**. Electron transfer, **d*** → **a** (or, **d** → **a***), then produces the charge-separated intermediate, I = [d^+,a^-], at rate constant, k_t. This intermediate can return to the ground state by the reverse electron-transfer process, $\mathbf{a}^- \rightarrow \mathbf{d}^+$, with rate constant, k_b. Within this scheme, the time course of the species A* and I are as follows:[4d]

$$A^*(t) = A^*(0)e^{-k_p t} \tag{1a}$$

$$I(t) = A^*(0)\left(\frac{k_t}{k_b - k_p}\right)(e^{-k_p t} - e^{-k_b t}) \tag{1b}$$

where $A^*(0)$ is the initial concentration of [**d***,**a**]. According to eq 1a, A* decays exponentially with rate constant,

$$k_p = k_D + k_t \tag{1c}$$

where k_D is the decay rate of A* in the absence of ET. Thus, k_t can be determined from k_p by independent measurement of k_D.

Equation 1b represents the creation of I from A* at a rate constant k_t and its reaction to form A at rate constant, k_b. This equation corresponds to an exponential rise and fall of I, with its concentration maximum at time τ: $I(\tau) = A^*(0)(k_t/k_>)\exp(-k_<\tau)$; $\tau = (\ln(k_>/k_<))/(k_> - k_<)$ where $k_>$ and $k_<$ refer to the

(1) (a) Mayo, S.; Ellis, W. R.; Crutchley, R. J.; Gray, H. B. *Science* **1986**, *233*, 948–952. (b) Marcus, R. A.; Sutin, N. *Biochim. Biophys. Acta* **1985**, *811*, 265–322. (c) Newton, M. D.; Sutin, N. *Annu. Rev. Phys. Chem.* **1984**, *35*, 437–480. (d) DeVault, D. *Quantum-Mechanical Tunnelling in Biological Systems*; Cambridge University Press: New York, 1984. (e) Mikkelsen, K.; Ratner, M. A. *Chem. Rev.* **1987**, *87*, 113.

(2) For example: (a) Miller, J. R.; Calcaterra, L. T.; Closs, G. L. *J. Am. Chem. Soc.* **1984**, *106*, 3047–3049. (b) Hush, N. S.; Paddon-Row, M. N.; Cotsaris, E.; Oevering, H.; Verhoeven, Z. W.; Heppner, M. *Chem. Phys. Lett.* **1985**, *117*, 8–11. (c) Heitele, H.; Michel-Beyerle, M. E. *J. Am. Chem. Soc.* **1985**, *107*, 8286–8288. (d) Isied, S. S.; Vassilian, A.; Magnuson, R. H.; Schwartz, H. A. *Ibid.* **1985**, *107*, 7432–7438. (e) Wasilewski, M. R.; Niemczyk, M. P. *ACS Symp. Ser.* **1986**, *No. 321*, 154.

(3) For example: (a) Kostic, N. M.; Margalit, R.; Che, C.-M.; Gray, H. B. *J. Am. Chem. Soc.* **1983**, *105*, 7765–7767. (b) Isied, S. S.; Kuehn, C.; Worosila, G. *Ibid.* **1984**, *106*, 1722–1726. (c) Nocera, D. G.; Winkler, J. R.; Yocom, K. M.; Bordignon, E.; Gray, H. B. *Ibid.* **1984**, *106*, 5145–5150. (d) Margalit, R.; Pecht, I.; Gray, H. B. *Ibid.* **1983**, *105*, 301–302. (e) Crutchley, R. J.; Ellis, W. R.; Gray, H. B. *Ibid.* **1985**, *107*, 5002–5004. (f) Bechtold, R.; Kuehn, C.; Lepre, C.; Isied, S. *Nature (London)* **1986**, *322*, 286–288. (g) Lieber, C. M.; Karas, J. L.; Gray, H. B. *J. Am. Chem. Soc.* **1987**, *109*, 3778–3779.

(4) (a) McGourty, J. L.; Blough, N. V.; Hoffman, B. M. *J. Am. Chem. Soc.* **1983**, *105*, 4470–4472. (b) Peterson-Kennedy, S. E.; McGourty, J. L.; Kalweit, J. A.; Hoffman, B. M. *Ibid.* **1986**, *108*, 1739–1746. (c) Ho, P. S.; Sutoris, C.; Liang, N.; Margoliash, E.; Hoffman, B. M. *Ibid.* **1985**, *107*, 1070–1071. (d) Liang, N.; Kang, C. H.; Ho, P. S.; Margoliash, E.; Hoffman, B. M. *Ibid.* **1986**, *108*, 4665–4666. (e) Liang, N.; Pielak, G. J.; Mauk, A. G.; Smith, M.; Hoffman, B. M. *Proc. Natl. Acad. Sci. U.S.A.* **1987**, *84*, 1249–1252.

(5) (a) Simolo, K. P.; McLendon, G. L.; Mauk, M. R.; Mauk, A. G. *J. Am. Chem. Soc.* **1984**, *106*, 5012–5013. (b) McLendon, G. L.; Winkler, J. R.; Nocera, D. G.; Mauk, M. R.; Mauk, A. G.; Gray, H. B. *Ibid.* **1985**, 739–740.

(6) (a) See: Dickerson, R. E.; Geis, I. *Hemoglobin*; Benjamin/Cummings: Menlo Park, CA, 1983. (b) Elber, R.; Karplus, M. *Science* **1987**, *235*, 318–321. (c) Fleming, G. R. *Chemical Applications of Ultrafast Spectroscopy*; Oxford, New York, 1986, pp 179 ff. (d) Northrup, S. H.; McCammon, J. A. *J. Am. Chem. Soc.* **1984**, *106*, 930–934. (e) Debrunner, P. G.; Frauenfelder, H. *Annu. Rev. Phys. Chem.* **1982**, *33*, 283–299. (f) Beece, D.; Eisenstein, L.; Frauenfelder, H.; Good, D.; Marden, M. C.; Reinisch, L.; Reynolds, A. H.; Sorenson, L. B.; Yue, K. T. *Biochemistry* **1980**, *19*, 5147–5157. (g) Frauenfelder, H.; Wolynes, P. *Science*, **1985**, *229*, 337–345. (h) McCammon, J. A.; Lee, C. Y.; Northrup, S. H. *J. Am. Chem. Soc.* **1983**, *105*, 2232.

0002-7863/87/1509-6237$01.50/0

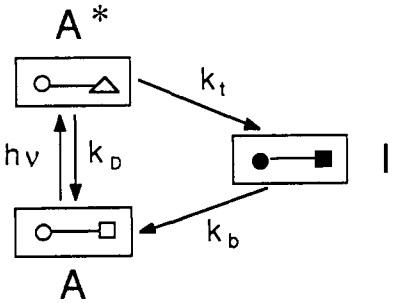

Figure 1. Simple kinetic scheme for electron transfer within a donor (□), acceptor (○) pair. State A represents the ground-state [**d**,**a**] pair. A* is the state formed at $t = 0$ by excitation to the donor excited state (△). State A* can decay back to A (rate constant, k_D) or can react to form the charge-transfer intermediate, I (rate constant, k_t), comprised of $\mathbf{d}^+$ (■) and $\mathbf{a}^-$ (●). In turn, reverse charge transfer regenerates A from I (rate constant, k_b).

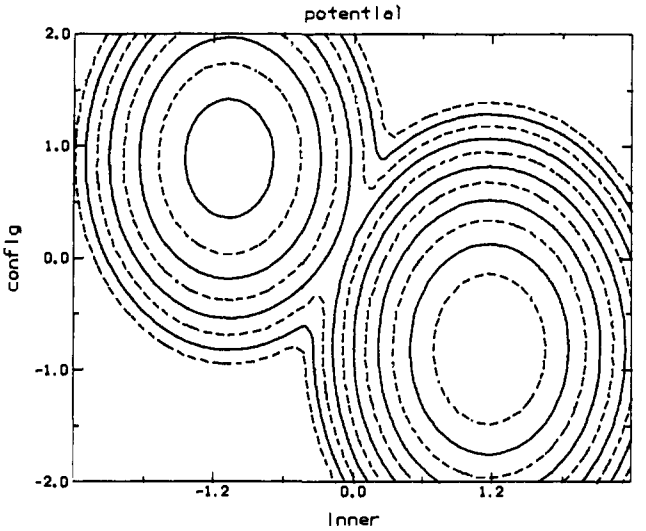

Figure 2. Schematic potential energy surface for ordinary electron transfer. The abcissa is the inner-sphere vibrational coordinate, the ordinate is either the outer-sphere coordinate or an internal low-frequency motion. The reaction proceeds over a saddle point located on a line joining precursor minimum (upper left) to successor minimum (lower right).

larger and smaller of k_b and k_t. If $k_b < k_p$, then k_b can be determined from the slow decay of intermediate I; if $k_b > k_p$, then k_b is obtained by measuring the rapid appearance of I.

The first portion of this scheme also applies to reactions where A* represents a state in which a rapid bimolecular event has reduced **d** or oxidized **a**. Such preparation can be done by pulse radiolysis or by flash photolysis of a sacrificial ET reagent;[1] a subsequent intramolecular charge-transfer step produces I as the end product. These two cases differ from the flash photolytic excitation of **d** (or **a**) in that $k_D = 0$.

II. Introduction of Conformational Variation

An electron-transfer event is controlled by the Franck–Condon principle, and thus is highly sensitive to the accompanying nuclear rearrangements. In the standard theory of Marcus and Hush,[1b,c] the coupled nuclear modes of motion are divided into inner- and outer-sphere modes. The former include bond-length changes in the redox centers themselves and contribute a reorganization energy, λ_i; the surrounding medium is treated as a continuous dielectric, with reorganization energy λ_0, and the total reorganization energy is $\lambda = \lambda_0 + \lambda_i$. A potential energy diagram depicting this situation is presented in Figure 2. In most cases, and particularly for small inorganic ions reacting near room temperature, inner- and outer-sphere reorganizations are treated on equal footing. Recently, however, it has been recognized that the dynamics of the outer sphere, or medium, can become important, and to date two types of consequences have been considered.

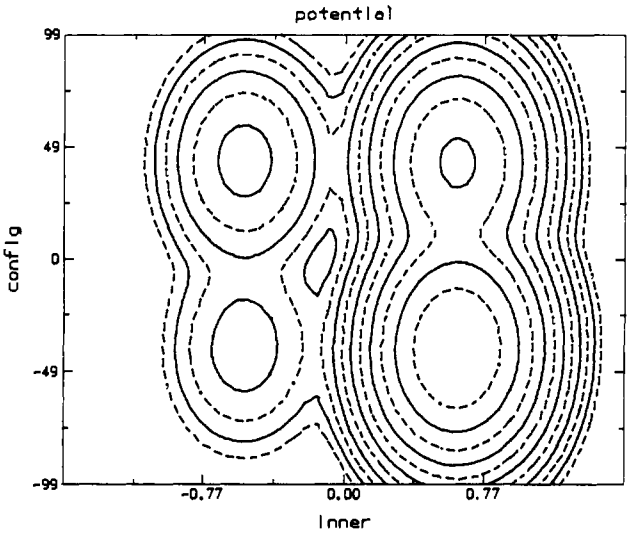

Figure 3. Schematic potential energy surface for electron transfer with conformational equilibrium. The ordinate is a conformational coordinate, and the surface describes processes such as the A* → I transfer described in the text and in Figure 4. Transfer from the conformationally favored precursor state (upper left) to the stable successor conformer (lower right) occurs by a two-step process (either across and then down or down and then across) rather than by the combined upper left to lower right path, which has a higher barrier.

(1) Traditional activated-complex theory assumes[1] that when the precursor species passes through the transition state, it goes on to form product with unit probability and with rate coefficient, kT/h. (a) Several authors recently have suggested that solvent relaxation is necessary to trap the successor species, which might otherwise convert back to precursor.[7] They therefore replace the prefactor kT/h by a rate τ_l^{-1} where τ_l is the longitudinal relaxation time of the medium.[7] (b) The activated-complex theory of reaction rates was extended long ago by Kramers, who considered the effects of slow (diffusive) motion along the reaction coordinate.[8] The Kramers approach replaces the universal prefactor kT/h of activated-complex theory by a form that is proportional to the friction (f) at low friction, and to f^{-1} at high friction. Several authors have applied such approaches to the ET problem and have shown, for instance, that reactions that would be nonadiabatic if considered on a purely energetic basis (insufficient time for electronic states to mix during nuclear passage through the transition state) can become adiabatic when frictional effects are included.[9] Some recent experimental work has confirmed the role of solvent dynamics.[10]

(2) Agmon and Hopfield[11] have further noted that for reactions in proteins it may be necessary to treat internal motion of the protein as defining the "medium" coordinate (Figure 2). When the protein is conformationally mobile, there are no new effects. However, as motion in this coordinate slows, reorganization in the protein coordinate becomes difficult and finally impossible; the system no longer can reach the classical transition state (Figure 2), the activation energy increases, and thus the electron-transfer

(7) (a) Kosower, E. M.; Huppert, D. *Annu. Rev. Phys. Chem.* **1986**, *37*, 127–156 and references therein. (b) McGuire, M.; McLendon, G. *J. Phys. Chem.* **1986**, *90*, 2549–2551.

(8) (a) Kramers, H. A. *Physica* **1940**, *7*, 284–304. (b) Carmeli, B.; Nitzan, A. *J. Chem. Phys.* **1984**, *76*, 5321–5333; **1986**, *80*, 3596–3605.

(9) (a) Hynes, J. T. *Annu. Rev. Phys. Chem.* **1985**, *36*, 573–597. (b) Skinner, J. L.; Wolynes, P. G. *J. Phys. Chem.* **1980**, *72*, 4913–4919. (c) Grote, R. F.; Hynes, J. T. *Ibid.* **1980**, *73*, 2715–2732. (d) van der Zwan, G.; Hynes, J. T. *Ibid.* **1983**, *78*, 4174–4185. (e) Calef, D. F.; Wolynes, P. G. *Ibid.* **1983**, *78*, 470–482. (f) Calef, D. F.; Wolynes, P. G. *J. Phys. Chem.* **1983**, *87*, 3387–3400. (g) Friedman, H. L.; Newton, M. D. *Faraday Discuss. Chem. Soc.* **1982**, *74*, 73–81. (h) Sumi, H.; Marcus, R. A. *J. Chem. Phys.* **1986**, *84*, 4272–4894. (i) Onuchic, J. N. *Ibid.* **1987**, *86*, 3925–3943.

(10) McManis, G. E.; Golovin, M. N.; Weaver, M. J. *J. Phys. Chem.* **1986**, *90*, 6563–6570 and references therein.

(11) (a) Agmon, N.; Hopfield, J. J. *J. Chem. Phys.* **1983**, *78*, 6947–6959. (b) Agmon, N.; Hopfield, J. J. *Ibid.* **1983**, *79*, 2042–2053.

Table I. Activation Energies[a]

	A* → I		I → A	
rate	k_{tC}	k_{tB}	k_{bC}	k_{bB}
ΔE^+	$[\lambda_t - \Delta E_t]^2/4\lambda_t$	$[\lambda_t - (\Delta E_t + \epsilon + \epsilon')]^2/4\lambda_t$	$[\lambda_b - \Delta E_b]^2/4\lambda_b$	$[\lambda_b - (\Delta E_b - \epsilon + \epsilon')]^2/4\lambda_b$

[a] Marcus–Hush activation energies for the rates constants defined in Figure 4. Reaction energies are used rather than free energies (ref 1); they are taken to be positive quantities and can differ for the A* → I and I → A processes as can the reorganization energies ($\lambda = \lambda_0 + \lambda_i$; see text), thus the subscripts, t or b.

rate decreases. The ET process in the absence of protein motion is equivalent to one with decreased exoergicity ($\Delta G° \rightarrow \Delta G° + \lambda_0$) and reorganization energy ($\lambda = \lambda_0 + \lambda_i \rightarrow \lambda_i$).[12]

All of these discussions assume that in both the "forward" ET process, A* → I, and back-transfer process, I → A, there is but a single stable conformational form of the precursor (P) and successor (S) electron-transfer states, namely, a single minimum in the medium, or outer-sphere, coordinate (Figure 2). However, it is quite clear that there must be many cases in which this coordinate has two minima (Figure 3), or more, and the substates of the P and S species display a dynamic conformational equilibrium that can modulate the ET rates.[13a] Consider our measurements of electron transfer within the complex between zinc cytochrome *c* peroxidase (ZnC*c*P) and cytochrome *c* (C*c*).[4] It is known that C*c* undergoes a structural change upon reduction,[14] and the same is likely to be true for C*c*P. Thus, it is to be expected that the complexes [ZnC*c*P,Fe^{III}C*c*] and [ZnC*c*P^+,Fe^{II}C*c*] have different conformations, and, as a result, electron transfer may be conformationally modulated. Moreover, it is well-established that major protein conformational changes even for systems of this size can occur at rates that are competitive with observed rates of ET.[13b] We have discussed the possibility that such "gating" may occur in this complex,[4d,e] as have Isied and his co-workers for C*c* itself.[3f] More generally, it has been proposed that a variety of other chemical reactions are conformationally gated.[6] In this paper, we treat a two-state case, which represents the simplest model for such reactions.

Consider for concreteness a donor/acceptor pair, [**d**,**a**], as part of a system that exhibits two conformations, B and C. For illustration we may imagine **d** and **a** attached 1,4 on a cyclohexane ring; the same formal situation will be realized in far more interesting ways with protein complexes. In this case, each of the three system states shown in Figure 1, (A, A*, and I) is comprised of two conformational substates ($A = A_B + A_C$; $A^* = A^*_B + A^*_C$; $I = I_B + I_C$). In the illustration, the distance and the through-bond relationships that govern electron transfer between **d** and **a** will differ in the boat (B) and chair (C) conformations of the ring. For nonadiabatic electron transfer, this would cause the matrix element that enters as a prefactor into the rate expressions to differ in the B and C conformers.[1] Generally, the energetics of charge creation or annihilation will be coupled to conformation; in the illustration this obviously occurs, for the coulomb stabilization of a charge-separated state will be greater in the boat conformer, where $\mathbf{d}^+$ and $\mathbf{a}^-$ are close, than in the chair. By linkage relationships, this means that the equilibrium between conformers is similar in system states A and A*, which have similar charge distribution, but differs in I. Interestingly, this direct coulomb–energetic coupling does not occur in charge-shift processes, where an electron or hole moves from one center to another, although the other coupling modes are unchanged.

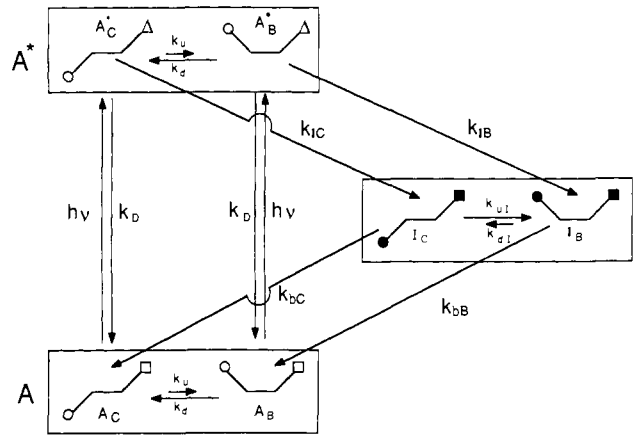

Figure 4. Kinetic scheme for electron transfer for a donor/acceptor couple within a system where the states A, A*, and I each undergoes conversion between two stable conformers C and B. The symbols and rate constants are as in Figure 1, with the following additions. The conformational substates and associated electron-transfer rate constants are labeled by conformer; rate constants are defined for the conformational conversion in A and A* ($k_u/k_d < 1$) and in I ($k_{u1}/k_{d1} > 1$).

Introduction of the conformational equilibrium implicit in Figure 3 expands the kinetic scheme of Figure 1 to that of Figure 4. Here, A, A*, and I states each exhibit two conformations of the linked donor/acceptor system, called B and C, with interconversion rates and energetics (equilibrium ratio) differing in I from those in A and A*. Moreover, the activation energy for ET is different for the two conformers; these energies are given in Table I where they are written to include the conformational energies explicitly.

This scheme includes ET rate constants only for the $\mathbf{d}^* \rightarrow \mathbf{a}$ and $\mathbf{a}^- \rightarrow \mathbf{d}^+$, electron-transfer processes in which the system conformation is conserved (the "horizontal" reactions in Figure 3), and conformational and ET steps only occur sequentially. Intuitively, it might be expected that a kinetic scheme for ET in the presence of an energetic coupling between charge state and conformation must include electron transfer that is synchronous with a conformational change in the medium coordinate, namely, the "diagonal" processes in Figure 3, $P_B \rightarrow S_C$ and $P_C \rightarrow S_B$. This in turn would open the issue of "friction" along the coupled, diagonal path, particularly in protein systems where large molecular masses are involved, and at low temperatures. However, it is *not* necessary to include the synchronous process, e.g., $A^*_C \rightarrow I_B$, for reasons that can be discerned upon examining Figure 3. On a potential energy surface in which the precursor, A* or I, and also the successor, I or A, exhibit two minima, the transition states on the diagonal reaction paths, e.g., P_C to S_B, *always* lie at a higher energy than all other transition states, those for the isoconformational ET reactions, $P_C \rightarrow S_C$ and $P_B \rightarrow S_B$, as well as those for the conformational conversions, $P_C \rightarrow P_B$ and $S_C \rightarrow S_B$ (Figure 3). There can be no compensation for this increased activation energy by the preexponential term when ET is adiabatic, nor is effective compensation feasible in the nonadiabatic, long-range ET processes of interest here. *Thus, the rates for the sequential conformational and ET processes always will be greater than those for the synchronous reactions, which can be omitted.* In some cases the conformational step will be the slower than the ET step, and these deserve to be called gated reactions. This point perhaps represents the most interesting feature of our analysis and will be shown below to have profound consequences for efforts to ascertain the degree of conformational control in electron-transfer reactions.[15,16]

(12) In their seminal papers Agmon and Hopfield assume that the reaction rate at fixed temperature is a function only of the protein coordinate. When applied to the ET problem, this simplification erroneously gives $\lambda = \lambda_0 + \lambda_i/2$ at high temperature.

(13) (a) An elegant discussion with respect to cytochrome *c* is given in: Williams, G.; Moore, G. R.; Williams, R. J. P. *Comments Inorg. Chem.* **1985**, *4*, 55–98. (b) For example, at pH 6 the T–R transition of hemoglobin has a rate constant, $k \sim 2 \times 10^4\ s^{-1}$: Marden, M. C.; Hazard, E. S.; Gibson, Q. H. *Biochemistry* **1986**, *25*, 7591–7596.

(14) (a) Takano, T.; Richardson, R. E. *J. Mol. Biol.* **1981**, *153*, 79–94. (b) Takano, T.; Richardson, R. E. *Ibid.* **1981**, *153*, 95–115.

(15) (a) In heterogeneous electron-transfer reactions there is a well-studied situation known as the "square scheme" that involves four stable states and in which it has been assumed without examination that synchronous processes need not be considered (ref 15b,c). Because of the difficulties involving treatment of mass transport only partial solutions to that more complicated problem are available. (b) Bond, A. M.; Oldham, K. B. *J. Phys. Chem.* **1983**, *87*, 2472–2502. (c) O'Connell, K. M.; Evans, D. H. *J. Am. Chem. Soc.* **1983**, *105*, 1473–1481.

III. Electron-Transfer Kinetics with Conformational Dynamics: Formal Analysis

We consider the kinetic scheme of Figure 4 and discuss it in terms of the photoinitiated, $\mathbf{d}^* \rightarrow \mathbf{a}$, electron transfer and thermal, $\mathbf{d}^+ \leftarrow \mathbf{a}^-$, processes in a donor/acceptor pair coupled within a molecule or complex that exhibits two stable conformations. As noted above, reactions initiated by a second-order reduction of **d** are described by the first half of this scheme. We define the population of A* in the C conformation as (A^*_C), in the B conformation as (A^*_B), and the total population of A* as (A*) ≡ (A^*_B) + (A^*_C). The population of the electron-transfer intermediate, I, and its conformational substates are defined analogously. In the ground and excited states, A and A*, the C conformer is more stable than B; for simplicity, we may write without loss

$$(A_B/A_C)_{eq} \cong (A^*_B/A^*_C)_{eq} = K_{eq} \equiv k_u/k_d = \exp(-\epsilon/kT) \ll 1$$

However, coupling between charge-state and conformation reverses the conformational equilibrium in I:

$$(I_B/I_C)_{eq} \equiv K^1_{eq} = k_{u1}/k_{d1} = \exp(+|\epsilon'|/kT) \gg 1$$

An important feature of most (but not all, e.g., ref 7a) experiments is that the detection methods employed do not distinguish between conformers. Thus, we require equations for the total populations, A* and I, following the formation of A* at $t = 0$ by flash excitation or second-order reduction of A. Generally, the $\mathbf{d}^* \rightarrow \mathbf{a}$ transfer process is experimentally characterized by following the loss of A*, the $\mathbf{d}^+ \leftarrow \mathbf{a}^-$ process by following the time course of I. We examine the two processes in turn.

A. Reaction of Initial State: A* → I. The kinetic schemes in Figure 3 and 4 correspond to the following kinetic equations for the A* populations:

$$\begin{aligned} d(A^*_C)/dt &= -(k_{tC} + k_u + k_D)(A^*_C) + k_d(A^*_B) \\ d(A^*_B)/dt &= k_u(A^*_C) - (k_{tB} + k_d + k_D)(A^*_B) \end{aligned} \quad (2a)$$

Because $K_{eq} \ll 1$, we may neglect A_B compared to A_C at the beginning of an experiment. Then the initial conditions for the A* state are $(A^*_C(0)) \equiv A^*_0$, $(A^*_B(0)) = 0$.

Steady-State Solution. The simplest kinetic analysis of these rate equations follows when it is appropriate to use the steady-state approximation for the higher energy conformer of the precursor, namely, the A^*_B, substate: $d(A^*_B)/dt = 0$. Defining k_{obsd} as an overall rate coefficient for the decay of A*, the above equations and their steady-state solution can be written

$$d(A^*)/dt = -k_{obsd}(A^*); \ (A^*) = A^*_0 e^{-k_{obsd}t} \quad (2b)$$

with

$$k_{obsd} = k_D + k^{ss} \quad (2c)$$

$$k^{ss} \doteq k_{tC} + k_{tB}\left(\frac{k_u}{k_{tB} + k_d + k_D}\right) \quad (2d)$$

where additional, smaller terms have been omitted from eq 2d. Thus, the steady-state solution of the kinetic scheme, Figure 4, for the A* → I process is formally equivalent to that in the simple scheme of Figure 1, eq 1a, with k_{obsd} (eq 2c) replacing k_p(eq 1c) and k^{ss} corresponding to k_t. The first term in k^{ss} arises from the direct process in which A^*_C formed by flash excitation decays to I_C, the second from the indirect process

$$A^*_C \xrightarrow{k_u} A^*_B \xrightarrow{k_{tB}} I_B$$

The two processes represent parallel channels for decay of the initial A* state and the two rate constants simply add. Under the assumption that $k_{eq} \ll 1$, the factor multiplying k_{tB} in eq 2d is $\ll 1$. Thus if the two conformers have similar reactivities, $k_{tB} \sim k_{tC}$, the conformational equilibrium will contribute little because of the low population of A^*_B; in eq 2d, $k^{ss} \sim k_{tC}$. However, if the C conformer is nonreactive, then reaction proceeds through A^*_B; in the limit of small k_{tC}, eq 2d becomes $k^{ss} \sim k_{tB}(k_u/(k_{tB} + k_d + k_D)) \ll k_{tB}$. The conformational gating then dominates the observed A* → I rate, and that rate is not simply the rate for an ET step.

Alternatively, if we consider a steady state in which the $A^*_C \leftrightarrow A^*_B$ conversion is faster than all other processes, then k_{ss} takes the form of a population-weighted average of the individual ET rates,

$$k_{ss} = \left(\frac{k_d}{k_u + k_d}\right)k_{tC} + \left(\frac{k_u}{k_u + k_d}\right)k_{tB} = f_C k_{tC} + f_B k_{tB} \quad (2e)$$

where f_i is the fractional occupancy of conformation A^*_i, $f_C + f_B = 1$, and in this instance we have relaxed the assumption that $K_{eq} \ll 1$.

Exact Solution. We also need to know what kinetic phenomena might be seen in the general case, where the steady state is not achieved. For example, while the steady-state condition holds, the equation for A*(t) (eq 2b) is formally identical with that for the ungated reaction (eq 1a), but there might be observable *direct* manifestations of gating at short time, as steady state is being approached, or at very long times. To achieve an exact solution of the kinetic scheme of Figure 4, we take sums and differences in eq 2a and obtain

$$\begin{aligned} d(A^*)/dt &= -k_+(A^*) + k_-(a^*) \\ d(a^*)/dt &= k_2(A^*) - k_1(a^*) \end{aligned} \quad (3a)$$

where $(a^*) = (A^*_C) - (A^*_B)$ and

$$\begin{aligned} k_\pm &= \tfrac{1}{2}(k_{tB} \pm k_{tC}) \qquad k_1 = k_+ + k_d + k_u \\ k_2 &= k_- + k_d - k_u \end{aligned} \quad (3b)$$

The coupled equation set (3a) can be solved by Laplace transform. Again, using the initial conditions $(A^*_C(0)) = A^*_0$, $(A^*_B(0)) = 0$, we find

$$(A^*) = c_1 e^{-ft} + c_2 e^{-gt} \quad (4)$$

with the definitions

$$2\{f,g\} = [k_u + k_d + k_{tB} + k_{tC} + 2k_D] \mp \sqrt{(k_u + k_d)^2 + 4k_2k_-} \quad (5)$$

$$c_1 = (k_1 + k_- - f)/(g - f) \quad (6a)$$

$$c_2 = (-k_1 - k_- + g)/(g - f) \quad (6b)$$

In contrast to the exponential dependence of A*(t) for the simple ET scheme (Figure 2, eq 1a) or for the steady-state solution to the conformational problem (Figure 4, eq 2b), the general form of the overall A*(t) population, eq 4, is biexponential, with the two rate constants being the sum (g) and difference (f) of two positive terms, $0 \le f \le g$. The long-time behavior of (A*) is governed by the rate constant, f, the short-time behavior by the larger rate constant, g. In the discussion below it will frequently be useful to consider situations where a single exponential controls the behavior of (A*(t)). As with the simple scheme (eq 1c) and with the steady-state solution to the full scheme (eq 2c), in every such case the effective rate, k_{obsd}, can be written as the sum of the decay rate constant, k_D, and an effective electron transfer term, k_{et},

$$k_{obsd} = k_D + k_{et} \quad (7)$$

There are several physically interesting limiting cases of eq 4–6.[17] The most interesting situation occurs when the state

(16) (a) In work to be published (ref 16b), Agmon and Kosloff have extended the treatment of Agmon and Hopfield (ref 11) to consider a case of multiple conformational minima. Based on a numerical solution of the 2-D diffusion to equation, they have noted that situations in which the reaction avoids synchronous pathways are generally favored. (b) Agmon, N.; Kosloff, R. *J. Chem. Phys.*, submitted for publication. We are grateful to the authors for a preprint of this work.

(17) One curious case, which might be called "anti-gating", arises if ET from A^*_B is ineffective, $k_{tB} \sim 0$ (Figure 4), but the $A^*_C \rightarrow A^*_B$ conformational conversion is permitted after formation of A^*_C. Here, the second conformation acts to reduce the overall ET rate by depleting the population of the active conformer.

initially prepared, A^*_C, does not exhibit rapid ET, $k_{tC} \sim 0$, and ET only occurs subsequent to the $A^*_C \rightarrow A^*_B$ conversion. This is "gated" ET in the traditional sense that until the "gate" has been opened, that is, until A^*_B is formed from A^*_C, there is no conversion to product, I. Equations 4–6 show that when the state, A^*_C, initially populated cannot undergo ET, there must be an initial lag period, with $k_{et} = 0$ (eq 7), the early-time ($t = 0$) rate constant for decay of A*,

$$k_{obsd} = k_D \tag{8a}$$

represents only the $A^*_C \rightarrow A_C$ return to ground state. Subsequently, k_{obsd} increases with time as A^*_B is formed and undergoes the $A^*_B \rightarrow I_B$ reaction.

In this gating situation, the long-time behavior of eq 4–6 exhibits two special cases of physical interest. When the conformational equilibrium is fast compared to the ET rate, corresponding to gated ET with a fast gate, at long time the $A^*_C \leftrightarrow A^*_B$ preequilibrium is established and we recover a version of the steady-state result, for $k_{tC} \approx 0$,

$$k_{obsd} \approx k_D + k_{tB}K_{eq} \tag{8b}$$

which is eq 2d when $(k_{tB} + k_D) \ll k_d$. Thus, the apparent electron-transfer rate k_{et} is reduced from k_{tB} by the factor $K_{eq} \ll 1$. The opposite extreme arises when conformational conversion $A^*_C \rightarrow A^*_B$ is slow compared to the subsequent ET; this is the traditional gated ET with a slow gate. At long time, the

$$A^*_C \xrightarrow{k_u} A^*_B$$

conformational step is rate limiting. Each complex attaining the high-energy conformation of the precursor crosses with essentially unit efficiency to the product state I; the overall ET rate constant is just $k_{et} = k_u$, and

$$k_{obsd} = k_D + k_u \tag{8c}$$

B. Reaction of ET Intermediate: I → A. The ET intermediate state denoted I in Figure 4 is created from A* and simultaneously is being converted to A by ET. The two conformers of A* can undergo parallel reactions to the corresponding I conformers. To illustrate simply the most important effects of gating on the kinetic behavior of the intermediate I, we take the dominant source of electronic state I to be the more stable A^*_C conformer; in effect we ignore gating in A* in order to see most clearly the effects of $I_B \leftrightarrow I_C$ conversion on the I → A process. As stated in section II, we take the coupling between charge state and conformation to reverse the relative stability of the B and C conformers on A* and I; the I_B state is the lower energy conformer of the ET intermediate. Also, in this section the term successor complex refers to A, and precursor complex is I.

With I formed only through I_C, the kinetic equations for the conformers of I are:

$$\begin{aligned} d(I_C)/dt &= k_{tC}e^{-k_{obsd}t} - (k_{bC} + k_{u1})(I_C) + k_{d1}(I_B) \\ d(I_B)/dt &= k_{u1}(I_C) - (k_{d1} + k_{bB})(I_B) \end{aligned} \tag{9}$$

Here $k_{obsd} = k_D + k_{tC}$ is the overall decay rate constant of the initial photoexcited state A*, (I_C) and (I_B) are populations of the high-energy and low-energy conformers of the I state of Figure 4 (shown as chair-like and boat-like, respectively). Denoting population sums and differences,

$$(I) = (I_C) + (I_B) \qquad (i) = (I_C) - (I_B) \tag{10}$$

the kinetic equations become

$$\begin{aligned} d(I)/dt &= k_{tC}e^{-k_{obsd}t} - k_{+}(I) + k_{-1}(i) \\ d(i)/dt &= k_{tC}e^{-k_{obsd}t} - k_{11}(i) + k_{21}(I) \end{aligned} \tag{11}$$

where the composite rate constants are defined by

$$\begin{aligned} k_{\pm 1} &= \tfrac{1}{2}(k_{bB} \pm k_{bC}) \qquad k_{11} = \tfrac{1}{2}(k_{bB} + k_{bC}) + k_{d1} + k_{u1} \\ k_{2I} &= k_{-1} + k_{d1} - k_{u1} \qquad k_{3I} = k_{bB} + k_d + k_u \end{aligned} \tag{12}$$

Once again, an exact solution is obtained by Laplace transform. Under the conditions discussed, namely, $A^*_C \rightarrow I_C$ as the only channel for creating I, the boundary conditions are $(I_C(t=0)) = 0 = (I_B(t=0))$, and the total population in the I electronic state at time t is

$$(I) = \frac{(-f^I + k_{31})}{(k_{obsd} - f^I)(g^I - f^I)}(e^{-f^I t} - e^{-k_{obsd}t}) + \frac{(-g^I + k_{31})}{(k_{obsd} - g^I)(g^I - f^I)}(e^{-k_{obsd}t} - e^{-g^I t}) \tag{13}$$

Here the composite constants g^I and f^I are defined as

$$2\{f^I, g^I\} = k_{u1} + k_{d1} + k_{bB} + k_{bC} \mp \sqrt{(k_{u1} + k_{d1})^2 + 4k_{21}k_{-1}} \tag{14}$$

The time course of (I) is determined by three exponentials involving the composite rate constants f^I, g^I, and the rate constant for the decay of A*, k_{obsd}.

To illustrate this exact description of the I → A process we examine the situation in which grating within I has the maximal effect: I is populated only through the $A^*_C \rightarrow I_C$ channel, but the I_C conformer to unreactive, with $k_{bC} = 0$. This represents idealized conformational control of ET because of the $\mathbf{d}^+ \leftarrow \mathbf{a}^-$ ET process can occur only after an $I_C \rightarrow I_B$ conversion through the sequential process

$$I_C \xrightarrow{k_{uI}} I_B \xrightarrow{k_{bB}} A$$

where the $I_C \rightarrow I_B$ step is the "gate". In this limit, eq 13 becomes

$$(I) = \frac{k_{obsd}k_{uI}}{(k_{obsd} - k_{bB})(k_{u1} - k_{bB})}(e^{-k_{bB}t} - e^{-k_{obsd}t}) + \frac{k_{obsd}k_{bB}}{(k_{obsd} - k_{u1})(k_{u1} - k_{bB})}(e^{-k_{obsd}t} - e^{-k_{u1}t}) \tag{15}$$

There are two interesting subcases. When the gating conformational change, $I_C \rightarrow I_B$, is slow compared to the rate of ET within the reactive B conformer ($k_{u1} \ll k_{bB}$),

$$(I) = \left(\frac{k_{obsd}}{k_{u1} - k_{obsd}}\right)(e^{-k_{obsd}t} - e^{-k_{u1}t}) \tag{16}$$

$$(k_{bC} = 0;\ k_{d1},\ k_{u1} \ll k_{bB})$$

When the gate is rapid compared to the subsequent ET step, then

$$(I) = \left(\frac{k_{obsd}}{k_{bB} - k_{obsd}}\right)(e^{-k_{obsd}t} - e^{-k_{bB}t}) \tag{17}$$

$$(k_{bC} = 0;\ k_{bB},\ k_{d1} \ll k_{u1})$$

Both of these subcases yield a biexponential functional form *identical* with that of the ungated kinetic scheme (eq 1b). One of the rate constants is k_{obsd}, associated with creation of I; the other describes the ET reaction, I → A. When the gate is slow, the apparent rate constant of the ET reaction is *not* that for the ET step, but rather is k_{u1}, a conformational parameter. Conversely, when the conformational change is fast, eq 17 says that the $\mathbf{d}^+ \leftarrow \mathbf{a}^-$ ET reaction within the I_B conformer is the rate-determining step for the I → A process.

Finally, note that gated ET, A* → I, with $k_{tC} = 0$ would initially populate I_B only. To the extent that A* decays with a single exponential, then the kinetic equations for the I → A process are obtained from eq 9–17 by a simple relabeling.

IV. Discussion

We have analyzed the simplest kinetic scheme for systems that display several stable conformational states and undergo intramolecular electron transfer. In particular, we have focused on the two-state situation in which the identity of the more stable state changes upon charge transfer: $K_{eq} = [A_B/A_C]_{eq}$, $[A^*_B/A^*_C]_{eq} < 1$, but $K^I_{eq} = [I_B/I_C]_{eq} > 1$. Despite this energetic coupling, we can omit the synchronous processes (e.g., $P_C \rightarrow S_B$) from consideration because the activation free energy along the

synchronous pathway always is greater than that for electron transfer within a single configuration. As we shall emphasize, the fact that ET and conformational reactions are sequential, and not concerted, is a major factor in efforts to disentangle conformational and electron-transfer influences. This is of key importance because standard detection methods monitor only the ET event, and not conformational changes within one electronic state: in many (most?) instances the measured time course of a gated ET reaction is predicted (section III) to be indistinguishable from a reaction without gating.

Consider first the A* → I reaction. With $k_D = 0$, this corresponds to the net reaction of system activated by a second-order redox process; with $k_D \neq 0$, this is the first step of photoinitiated ET (Figure 4). In all the individual cases considered, the A* → I reaction is predicted to exhibit a simple exponential decay over most of its time course. Thus, without independent information about rates of conformational change, it is not possible to deduce from a single such experiment whether the decay is influenced by a conformational process. Only *if* it is possible to observe a lag or a burst at *short* time, might such a discrimination be possible.

Now consider the I → A reaction, the decay of the electron-transfer intermediate formed by a photostimulated electron transfer. In the limiting cases (eq 16 and 17), the time course of I corresponds to an exponential rise and fall. One of the two exponentials is associated with the A* → I process, the other with I → A, and the results are formally indistinguishable from those obtained in the absence of gating (eq 1b). Again, the rate constant governing I → A can reflect either the $I_C \rightarrow I_B$ conversion (eq 16) or the actual ET step (eq 17). Clearly, provided that we measure only $I(t)$ and not $i(t)$, there is no way to characterize the role of conformational change in determining the rate constant for the decay of I from a single kinetic measurement. Of course, the general solution to the kinetic problem is more complicated, involving terms that are composites of ET and conformational constants (eq 13). However, we expect that there will be many cases where experimental signal/noise will be inadequate to distinguish convincingly the general behavior from the limiting form, and in any case, two composite rate constants do not specify those for all elementary processes (Figure 4).

Fortunately, the partial decoupling of ET and conformational processes afforded by the absence of synchronous events in principle *and in practice* allows for the identification of an observed decay rate constant. If one constructs a series of homologous systems in which the ET energetics (or electronic coupling) is modified *without* change in the conformational equilibrium, thus leaving the conformational rates unchanged, then the *observed* rate constants will be unchanged if the reaction is controlled by a conformational rate, but will vary if this is not so.

Consider the A* → I process, as represented by the reduction, say, of met-Mb by $Ru^{II}(L)_5$ covalently attached to a surface histidine.[3e] In the initial experiments L = NH_3 and the observed rates of ET are slow, $k_{et} < 0.1\ s^{-1}$. Thus, it could be argued that this might represent *not* the rate for long-distance ET, but rather the rate for a protein fluctuation large enough to permit the $Ru^{II}(NH_3)_5$ to "swim" close enough to the heme iron that it can rapidly react; in this case the reaction would be described by eq 8c where $k_{obsd} = k_u$ (recall, $k_D = 0$ in this experiment). Even the observation of different rates for attachment of Ru at different sites[1a] at unequal distances from the heme is not adequate to disprove such a contention, for it is to be expected that different breathing motions will be required to allow penetration from different points on a protein's surface. However, by chemical modification of the attached reagent (say by using $Ru^{II}(NH_3)_{5-x}(L)_x$ where L can be pyridine or isonicotinamide, or $(L)_2$ = bipy or a substituted bipy, or L_x is any other of the myriads of available ligands), it is possible to make a series of substitutions that change the energetics of ET, but not the conformational influence of the attached Ru complex. Data obtained to date indicate that k_{obsd} does vary with such changes,[3f,g] and thus we may conclude that eq 8c does not apply and that k_{obsd} is an electron-transfer quantity and is *not* controlled simply by a slow conformational gate. Rapid conformational equilibrium is not ruled out. For example, if the Ru complex shuttles rapidly between two adjacent positions on the protein's surface, the rate constant would be a weighted average, and eq 2d or 2e would obtain. Fortunately, the existence of such states and conversion between them can be addressed directly by spectroscopic probes.[18]

Now consider the I → A process, as represented by the Fe^{II}Por → ($ZnPor^+$) electron transfer within the [ZnC*c*P$^+$, C*c*] charge-separated intermediate that is formed by the photostimulated ^{3}ZnPor → Fe^{III}Por forward process.[4,5] We have found recently that the observed time course for the intermediate I can be described by eq 1b, and that the ET rate constant, k_b, varies by three orders of magnitude, depending on the species of C*c* employed.[4d] Even more dramatic, by changing a single amino acid residue, Phe-87 of yeast C*c*, this rate constant can be changed by four orders of magnitude![4e] Do these changes represent modifications of a gating process, representative of the fact the [ZnC*c*P, Cc^{III}] complex has a different structure from that of the [ZnC*c*P$^+$, Cc^{II}] complex or, in the opposite limit, might they represent changes in the ET rate within a single conformation?

As shown above, intermediate I can be described by equations similar to eq 1b in the presence of a conformational equilibrium, but the effective k_b can either be an electron transfer rate (eq 17) *or* a conformational rate[1] (eq 16). Focusing on the experiments in which Phe-87 is varied, if an ET rate dominates and the aromatic residue is indeed important because it increases the electronic matrix element coupling donor and acceptor, then this would contribute to the preexponential term of k_{bC}, and one would predict the activation energy to be unaffected by the substitution. Thus, a study of temperature dependences will be informative.

A more direct probe of this reaction will, again, be to vary the energetics of the ET process for each of the wild-type and mutant C*c*, without changing their conformational preferences. Clearly, this is best done by a change in the C*c*P partner. By reconstituting C*c*P with MgPor and with Zn and Mg porphyrins substituted at the periphery of the macrocycle, the redox potential of the metalloporphyrin, both in excited and ground states, can be varied without modifying the conformational properties of C*c*P. By comparing the observed ET rates for each of the wild-type and mutant C*c* with, say ZnC*c*P and MgC*c*P, there is a strong possibility that we can unambiguously identify the phenomenon that underlies the 10^4-fold rate discrimination.

V. Concluding Remarks

With the aims of specificity and clarity, we have discussed conformational effects in terms of intramolecular electron-transfer phenomena, focusing on a donor–acceptor complex activated by flash photolysis or a second-order redox event. The general set of rate equations (eq 2a and 9) and the kinetic scheme of Figure 4, however, are applicable to other types of rate process. For example, either proton transfer or isomerization reactions can be controlled by gating, that is, by conversion between two conformational geometries that have different reactivities. The presence of additional minima on a two-dimensional potential energy surface that involves a conformational coordinate (the vertical coordinate of Figure 4) distinguishes this class of reactions. As pointed out in section II, a key feature of processes that involve such additional conformational minima is that the "diagonal" path (upper left to lower right in Figure 3), involving concerted change of conformational and electronic states, always has a higher activation energy than the sequential processes in which either conformational or electronic change occurs first. Thus, the system will avoid the high activation-energy "diagonal" path; this increases the overall rate yet provides an elegant gating mechanism through conformational change. Gated conformational control apparently is quite common in biological ET situations, and is becoming of increasing interest in ET reactions, involving such systems as micelles, photoelectrochemical and photochemical conversion schemes, and donor–acceptor species. Consideration of gated processes further

(18) For example: Gummin, D. D.; Ratilla, E. M. A.; Kostic, N. M. *Inorg. Chem.* **1986**, *25*, 2429–2433.

suggests alternative interpretations of many reactions (gasification, cyclization, hydrogenation, etc.) that involve conformational conversion.

Acknowledgment. We acknowledge stimulating discussions of ET processes with Professor A. Nitzan, J. Hupp, and H. B. Gray. This work has been supported by the National Institutes of Health (HL 13531; B.M.H.), the National Science Foundation (DBM86-06575, B.M.H.), and the Basic Coal Sciences Program of the Gas Research Institute (M.A.R.).

Infrared Spectra of the NH_3-F_2 and NH_2F-HF Complexes in Solid Argon

Lester Andrews* and Robert Lascola

Contribution from the Chemistry Department, University of Virginia, Charlottesville, Virginia 22901. *Received March 26, 1987*

Abstract: Cocondensation of Ar/NH_3 and Ar/F_2 samples at 12 K produced a weak NH_3-F_2 complex, which photolyzed to give several NH_2F-HF complexes, based on matrix infrared spectra. The major product contained HF hydrogen bonded to the nitrogen lone pair of NH_2F and exhibited ν_s(HF) = 3389 cm^{-1} and ν_l(HF) = 750 and 723 cm^{-1}; these observations characterize a weaker H_2FN-HF interaction than the H_3N-HF interaction and indicate weaker basicity for NH_2F than NH_3. Four NH_2F submolecule modes observed for the complex provide the first direct spectroscopic evidence for the highly reactive NH_2F molecule. The minor product exhibited HF bonded to a fluorine lone pair with ν_s(HF) = 3722 cm^{-1} and ν_l(HF) = 596 and 515 cm^{-1}; this spectrum characterizes a stronger interaction for NH_2F-HF than for CH_3F-HF.

Fluoramide is the simplest and perhaps the most elusive substituted amine owing to extremely high reactivity. Although there is no report of isolation or characterization of NH_2F in the literature, NH_2F has been generated from various media and postulated as a reaction intermediate[1-5] and subjected to theoretical calculations of structure,[6-8] infrared spectra,[9] inversion barrier,[10-12] and proton affinity.[13,14] In the most recent study $(NH_3F^+)(HF_2^-)(HF)_n$ salts were sublimed under vacuum, and 16-eV electron impact produced a strong mass 35 peak, which provides evidence for the evaporation of NH_2F molecules.[5] Fluorimide (NHF_2), however, is relatively stable in the gas phase, and its infrared spectrum has been recorded,[16] but under certain conditions it can be a vicious explosive.[17] Matrix photochemical reaction of the CH_4-F_2 dimer produced the CH_3F-HF complex,[18] and the analogous NH_3-F_2 matrix photochemical reaction was performed in an attempt to stabilize and characterize fluoramide in the NH_2F-HF complex. This complex follows a series of HF complexes with NH_3, alkylamines, and hydroxylamine studied in this laboratory[19-21] and compares the effect of a fluorine substituent on the spectrum of the HF complex.

Table I. New Absorptions (cm^{-1}) Observed on Cocondensation, Photolysis, and Annealing of Ar/NH_3 and Ar/F_2 Samples at 12 K[a]

$NH_3 + F_2$	$^{15}NH_3 + F_2$	NHD_2	$ND_3 + F_2$	ident.
3722	3722	3718	2735	ν_s(F) (**2**)
3626	3626	3611	2652	ν_s (**3**)
3450	3448	3452	2548	site of **1**
3389	3388	3384	2505	ν_s (**1**)
3269	3264		2399	ν_l (**1**)
3063	3063			NH_2-HF
1568.1	1565.9	1428.9[b]	1151.4	ν_2 (**1**)
1314	1314	1312	998	$2\nu_l$ (**1**)
1243.7	1238.0	979.7	968.1	ν_2 (**1**)
966.2	962.2		748.3	NH_3-F_2
933.7	916.2	933.4	923.7	ν_3 (**1**)
781.0	781.0	obscured		NH_3-F_2
750.3	750.3	738.8[c]	560.9[d]	ν_l (in-plane) (**1**)
723.0	723.0	725.0	539.9	ν_l (out-plane) (**1**)
596.7	597.0	596	441	ν_l(F) (**2**)
514.7	514.6	515	381	ν_l(F) (**2**)

[a] Very weak bands for NH_3-HF (ref 17) are not included. [b] Absorption for NHDF-HF; other sharp bands for this mixed isotopic species appeared at 1209.2 and 1015.3 cm^{-1}. [c] Due to ν_l(HF) in ND_2-F-HF. [d] Shoulder at 567.0 cm^{-1} due to ν_l(DF) in NHDF-DF.

Experimental Section

The matrix photolysis experiments involved a combination of techniques applied in other studies.[18,19] Ammonia (Matheson) and ND_3 and $^{15}NH_3$ (MSD isotopes) were diluted with argon to 200/1 or 400/1 ratios. Fluorine (Matheson) was mixed with argon to 100/1 or 200/1 ratios in a passivated stainless-steel system, and in some experiments, this sample was passed through a U-tube immersed in liquid nitrogen to remove HF before deposition. Samples were codeposited at 3-4 mmol/h each for

(1) Homann, K. H.; McLean, D. I. *Ber. Bunsenges. Phys. Chem.* **1971**, *75*, 945.
(2) King, R. T. V.; Roberts, R. *J. Phys. Chem.* **1974**, *78*, 1433 and references therein.
(3) Grakauskas, V.; Remanick, A. H.; Baum, K. *J. Am. Chem. Soc.* **1968**, *90*, 3839. Grakauskas, V. *J. Inorg. Nucl. Chem.* **1973**, *35*, 3034.
(4) Jonder, J.; Muench, V. *Z. Anorg. Allg. Chem.* **1978**, *446*, 193.
(5) Minkwitz, R.; Liedtke, A.; Nass, R. *J. Fluorine Chem.* **1987**, *37*, 307.
(6) Gordon, M. S.; Pople, J. A. *J. Chem. Soc., Chem. Commun.* **1970**, 1062.
(7) Keil, F.; Kutzelnigg, W. *J. Am. Chem. Soc.* **1975**, *97*, 3623.
(8) Pople, J. A.; Raghavachari, K.; Frisch, M. J.; Binkley, J. S.; Schleyer, P. v. R. *J. Am. Chem. Soc.* **1983**, *105*, 6389.
(9) Fogarasi, G.; Pulay, P.; Molt, K.; Sawodny, W. *Mol. Phys.* **1977**, *33*, 1565.
(10) Lehn, J. M.; Munsch, B. *J. Chem. Soc., Chem. Commun.* **1970**, 1062.
(11) Schmiedekamp, A.; Skaarup, S.; Paulay, P.; Boggs, J. A. *J. Chem. Phys.* **1977**, *66*, 5769.
(12) Yabushita, S.; Gordon, M. S. *Chem. Phys. Lett.* **1985**, *117*, 321.
(13) Johansson, A.; Kollman, P. A.; Liebman, J. F.; Rothenberg, S. *J. Am. Chem. Soc.* **1974**, *96*, 3750.
(14) Del Bene, J. E.; Frisch, M. J.; Raghavachari, K.; Pople, J. A. *J. Phys. Chem.* **1982**, *86*, 1529.
(15) Kennedy, A.; Colburn, C. B. *J. Am. Chem. Soc.* **1959**, *81*, 2906.
(16) Comeford, J. J.; Mann, D. E.; Schoen, L. J.; Lide, D. R., Jr. *J. Chem. Phys.* **1963**, *38*, 461.
(17) Christe, K. O.; Wilson, R. D. *Inorg. Chem.* **1987**, *26*, 920.
(18) Johnson, G. L.; Andrews, L. *J. Am. Chem. Soc.* **1980**, *102*, 5736.
(19) Johnson, G. L.; Andrews, L. *J. Am. Chem. Soc.* **1982**, *104*, 3043.
(20) Andrews, L.; Davis, S. R.; Johnson, G. L. *J. Phys. Chem.* **1986**, *90*, 4273.
(21) Lascola, R.; Andrews, L. *J. Am. Chem. Soc.* **1987**, *109*, 4765.

0002-7863/87/1509-6243$01.50/0